

## The Effect of the Phonon Drag on the Seebeck Coefficient in SiC

Vitalijus BIKBAJEVAS\*, Vytautas GRIVICKAS

*Institute of Materials Science and Applied Research, Vilnius University, Saulėtekio 10, LT-10223 Vilnius, Lithuania*

*Received 08 October 2004; accepted 13 October 2004*

The Seebeck coefficient study in 4H- and 6H- is presented. The Seebeck coefficient steeply increases with decreasing temperature. This behavior is assigned to the phonon drag effect. An approach to the theoretical modeling of the phonon drag effect is discussed and simulation of the Seebeck coefficient temperature-dependence is displayed.

*Keywords:* thermopower, Seebeck coefficient, phonon drag effect, SiC.

### INTRODUCTION

The Seebeck effect involves the voltage produced across two points of the material(s) when they are at different temperatures. It can be easily observed and Seebeck effect is widely used for determination of the free carrier charge sign. The Seebeck coefficient,  $S$ , is defined as the limit of the quotient of the voltage,  $U$ , generated between the two points divided by the difference of their temperature,  $\Delta T$ , e. i.  $S = U/\Delta T$  as  $\Delta T$  approaches zero. The magnitude of the Seebeck coefficient is related to the charge carrier scattering type in the material and to the density-of-state effective mass of the charge carriers. Hence, if one of the two mentioned quantities is known information about the other could be obtained. More recently it was found out that apart from classical free carriers diffusion the part of so-called photon drag phenomenon contributes significantly to the Seebeck effect especially at low temperatures [1]. The photon drag effect consists in a 'carrying' of electrons by long wavelength phonon current created by temperature gradient. In fact this effect is due to an asymmetrical scattering of the electron current by the lattice vibrations, i.e. charge carriers are preferentially pushed towards the cold end of the sample. It should be particularly emphasized that the Seebeck coefficient appears as a factor in the equation term describing any nonisothermal part of actual semiconductor devices and, thus, must be included properly during the device modelling.

The Seebeck effect in some SiC polytypes was investigated in sixties and seventies. At that time, it was observed that in SiC the Seebeck coefficient exceeds the ones in silicon and germanium. It was believed that the reason for that phenomenon was not only in a simple difference in the bandgap energy but also in a stronger phonon drag effect. However, in those early investigations the polytype of SiC, the carrier concentration and many transport parameters of the semiconductor were not specified accurately enough.

Some of the SiC polytypes are currently among the most attractive candidates for electronics designed to operate under harsh conditions including high

temperatures [2]. Therefore, determination of the Seebeck coefficient for SiC is of great importance.

In this work, we have obtained the Seebeck coefficient for well-defined  $n$ -4H- [3] and  $p$ -6H-SiC [4] crystal. In addition, some results from the article [5] for  $n$ -6H-SiC are also present for Seebeck coefficient was determined in a wide range of the free electron concentration. Ref. 4 was published in Russian in such journal that remains unknown for a wide scientific community. Furthermore, in our article theoretical modeling of the phonon drag effect is discussed and simulation of the Seebeck coefficient temperature dependence is displayed.

### EXPERIMENTAL DETAILS

#### Samples

**$n$ -4H-SiC.** A 300- $\mu\text{m}$  thick epilayer of  $n$ -type nitrogen doped 4H-SiC was grown on a substrate by the sublimation technique [6]. Then the substrate was carefully polished away and Ti contacts were deposited and annealed for 5 min. at 950 °C.

**$p$ -6H-SiC.** These samples were cut out from the bulk  $p$ -6H-SiC single crystal. Two types of the samples were used in the investigation: cut parallel and perpendicular to  $c$ -axis of SiC crystal. The concentrations of the impurities in the samples obtained using SIMS are presented in Table 1.

**Table 1.** Impurities in  $p$ -6H-SiC obtained by SIMS

Impurity	Concentration ( $\text{cm}^{-3}$ )
B	$3 \cdot 10^{17}$
Al	$1.5 \cdot 10^{16}$
V	$2 \cdot 10^{16}$
Ti	$4 \cdot 10^{17}$

**$n$ -6H-SiC** [5]. Samples of  $n$ -6H-SiC:N were cut out in the shape of parallelepiped from the single 6H-SiC crystal perpendicular to  $c$ -axis. Ohmic contacts were deposited by alloying Au+Ta in vacuum. Various doped samples were used in this study. We take only 3 of them: low, middle and high doped ( $n = 1.1 \times 10^{15}$ ,  $1.5 \times 10^{16}$  and  $3.8 \times 10^{17} \text{ cm}^{-3}$  at 100 K, respectively).

\*Corresponding author. Tel.: +370-5-2698725; fax: +370-5-2698690.  
E-mail address: vitalijus.bikbajevs@ff.vu.lt (V. Bikbajevs)

## Thermopower measurement

A typical experimental determination of the Seebeck coefficient follows its definition. A small temperature difference between two ends of the sample is maintained and the voltage drop between them is measured. Accurate measurements require a very careful sample contact preparation and well-defined thermal conditions.

A sample holder used in our experiment consists of a fork-like body with two symmetrical contact blocks that carried a sample and can be heated by low-power subheaters. The blocks serve both as heat and electrical contact for simultaneous thermopower and Hall effect measurement. The sample holder is surrounded by a radiation screen and placed in a cryostat. The temperature of the holder can be changed in the range 85 – 400 K. The Copper – Constantan (Cu/Ni) thermocouples serve as voltage probes and temperature sensors at the same time. Pressure contacts were used for thermocouples and heat sinks.

A sophisticated measurement procedure for determining of the Seebeck coefficient was implemented. It is based on the alternative use of two subheaters and the recording of all thermal voltages. Such method makes it possible to eliminate errors caused by bad thermal contact, parasitic heat flux through thermocouple, low heat conducting or inhomogeneous samples, etc. The thermopower voltage was measured under nearly steady state conditions maintaining a small positive and negative temperature drop  $\Delta T$  between the ends of the sample. The measured voltages actually depend on the difference in the Seebeck coefficients of the semiconductor sample and the thermocouple wires since they are also experiencing the temperature drop. The double simultaneous measurements using Copper ( $U_{Cu}$ ) and Constantan ( $U_{Con}$ ) as contact wires allow extracting the Seebeck coefficient of the sample. Any nonlinear temperature distribution and an inhomogeneous Seebeck coefficient lead to additional spurious voltage ( $U_e$ ) between ‘hot’ and ‘cold’ ends of the sample measured in Copper and Constantan circuit.  $U_e$  is independent of temperature difference  $\Delta T$  and can be eliminated if the relationship  $U_{Cu}$ ,  $U_{Con}$  vs.  $\Delta T$  is known. So, the dependence  $U_{Cu}(\Delta T)$  and  $U_{Con}(\Delta T)$  has been obtained at every temperature point. The detail procedure of Seebeck coefficient extracting from the measured parameters can be found in Ref. 7. An example of such measurement

in  $n$ -4H-SiC at  $T=401$  K is presented in Fig. 1. Small spurious voltage ( $U_e$ ) is evident at  $\Delta T=0$ . Two slopes ( $a_1$  and  $a_2$ ) allow accurate extraction of the Seebeck coefficient

( $S=-0.56$  mV/K in particular case shown in Fig. 1). The measurements of the Hall effect have been performed simultaneously with Seebeck coefficient.

## RESULTS AND DISCUSSION

### $n$ -4H-SiC

The dependencies of free electron concentration and their mobility vs. temperature in  $n$ -4H-SiC are presented in

Fig. 2. Some data of similarly doped 4H-SiC from literature are also shown in order to illustrate the influence

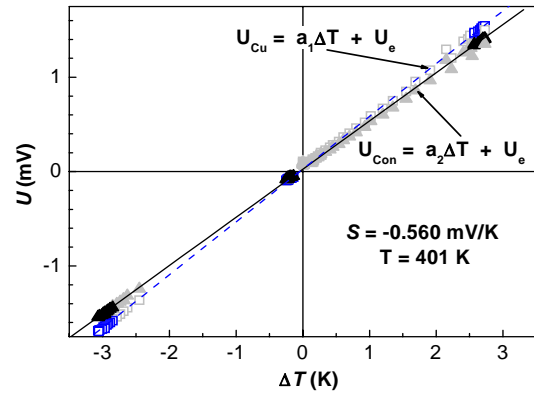


Fig. 1. Evaluation of voltage slopes for calculating  $S$

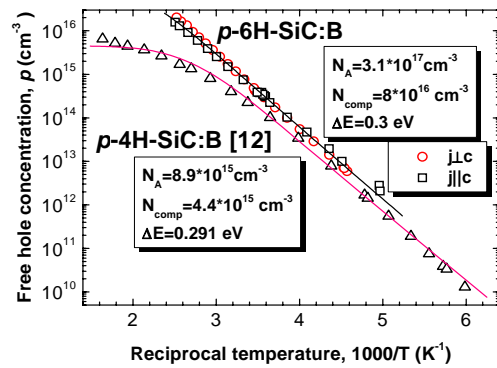


Fig. 2. Temperature dependence of the free electron concentration in  $n$ -4H-SiC. The line indicates the neutrality equation with presented parameters

of the doping on free electron concentration and their mobility. Nitrogen atoms are donors in these samples. They can occupy position in hexagonal or cubic sites. Therefore, nitrogen donors form two donor levels with not too much different activation energies [10]. However, as one can see in Fig. 2 we were able to fit temperature electron concentration dependencies using single donor activation energy. We have estimated the total donor concentration in our samples as  $6 \times 10^{18} \text{ cm}^{-3}$  and concentration of compensating acceptors to be  $1 \times 10^{17} \text{ cm}^{-3}$ . The temperature mobility dependencies for the same samples as in Fig. 2 are presented in Fig. 3. The main difference among three presented samples is concentration of the impurities. As it was found in [11] the dominant scattering mechanisms in  $n$ -type 4H- and 6H-SiC are ionized impurity scattering, acoustic phonon and intervalley scattering for the low-, intermediate- and high-temperature regions, respectively. Furthermore, the authors of Ref. 11 obtained that  $n$ -4H-SiC in the configuration  $\mathbf{B}||\hat{c}$  and  $\mathbf{j}\perp\hat{c}$  mobility determined by ionized impurity scattering  $\mu_{ion} \sim T$ , by acoustic phonons impurity scattering  $\mu_{ac} \sim T^{-1.5}$  and by intervalley scattering  $\mu_{ac} \sim \exp(-E/kT)$ . Inspection of the curves in Fig. 3 shows that the main scattering mechanisms of free electrons in our samples is likely to be ionized impurity scattering.

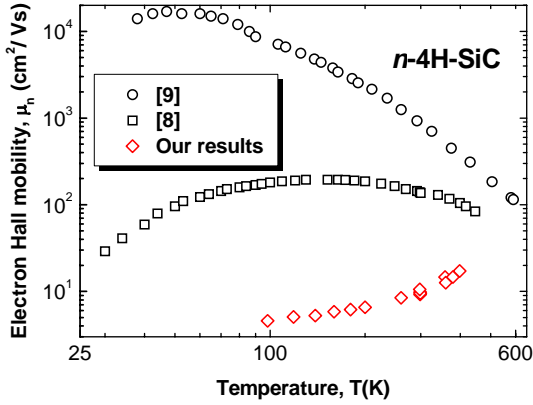


Fig. 3. Temperature dependence of the Hall mobility in *n*-4H-SiC

### *p*-6H-SiC

The temperature concentration dependence of *p*-6H-SiC samples is presented in Fig. 4. The parameters of the fitting curve are also present. There were two types of the *p*-6H-SiC samples, namely parallel and perpendicular to SiC crystal  $\hat{c}$ -axis. However, in all our measurements (concentration, mobility, Seebeck coefficient) the difference between values of such parameters in two types of the samples was within the experimental error. So, in our investigation we failed to obtain discrepancy in the behavior samples parallel and perpendicular to  $\hat{c}$ -axis. The fitting curve has been calculated using the neutrality equation for a nondegenerate *p*-type semiconductor with single acceptor level [12]. The parameters of the fitting curve are presented in Fig. 4. The obtained concentration of the acceptors ( $3.1 \times 10^{17} \text{ cm}^{-3}$ ) is in good agreement with Boron concentration ( $3 \times 10^{17} \text{ cm}^{-3}$ ) derived from SIMS (see Table 1). The obtained activation energy  $\Delta E_A = 0.30 \text{ eV}$  is also in good agreement with the same energy values of Boron-related centers in *p*-6H-SiC from literature [10, 13]. Quite small free carrier and large compensating atoms concentrations are evidence of strong semiconductor compensation.

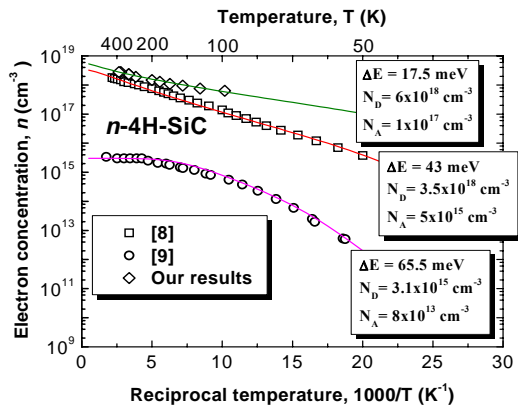


Fig. 4. Temperature dependence of the free hole concentration in our *p*-6H-SiC and B doped *p*-4H-SiC from Ref. 12

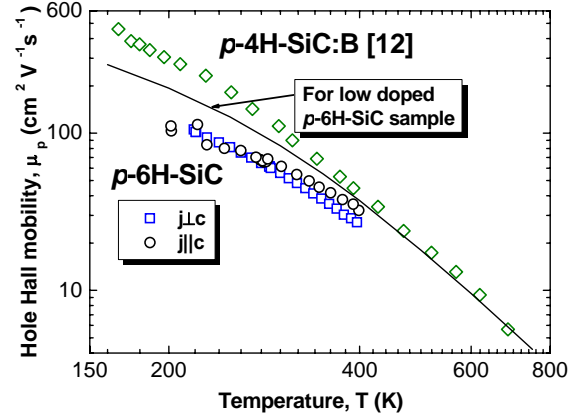


Fig. 5. Temperature dependence of the Hall mobility

Fig. 5 represents mobility vs. temperature. We failed to find mobility temperature dependence for *p*-6H-SiC in literature. There are only very few values of the hole mobility in this polytype of SiC at room temperature [14, 15]. By recognizing that the structure of the valence band in 6H- and 4H-SiC is very similar we assumed that free carrier scattering mechanisms operate in the same manner in both cases. Furthermore, the hole mobility at room temperature in 4H-SiC is 20 – 30 % higher than in 6H- over wide range of impurity concentration [15]. So, assuming the mobility in 6H-SiC:B as 75 % of that in 4H-SiC with the same Boron concentration ( $8.9 \times 10^{15} \text{ cm}^{-3}$  [12]), we present  $\mu_p$  by solid line (Fig. 5). Our samples are stronger doped and their mobility is lower. As it was found in Ref. 11 the dominant scattering mechanisms in *n*-type 4H- and 6H-SiC are ionized impurity scattering, acoustic phonon scattering and intervalley scattering for the low-, intermediate- and high-temperature regions, respectively. The acceptors activation energy in *p*-type SiC (0.2 – 0.3 eV) is greater than donors activation energy in *n*-SiC and hence sufficiently large amount of dopant atoms are in neutral state. In this case neutral impurity scattering can be important for acceptor concentration above  $10^{16} \text{ cm}^{-3}$  [16]. However, the form of the temperature mobility dependence in the range 400 – 100 K testifies that the main free holes scattering mechanism, which determines their mobility is acoustic phonon scattering.

### *n*-6H-SiC [3]]

The values of free electron concentration in *n*-6H-SiC were determined only at two temperatures 100 and 500 K. They are presented in Fig. 6 together with the other *n*-T dependencies from literature to be certain that Kirsons' data [5] are actual. Moreover, temperature dependencies of the samples from Ref. 10 allow us to imagine possible mobility vs. temperature relationship of Kirsons' samples (Fig. 7).

### Seebeck coefficient

The temperature dependence of the Seebeck coefficients is shown in Fig. 8 and 9. In all cases the Seebeck coefficient increases with decreasing temperature.

Furthermore, the value of the thermopower highly depends on the sample doping and Seebeck coefficient strongly reduces with increasing of doping (Fig. 9).

The thermopower consists of two components: diffusion and phonon (phonon drag effect) and can be presented as a sum of them  $S = S_{e[h]} + S_{ph}$ . Diffusion part for non-generated semiconductor can be expressed as [1]:

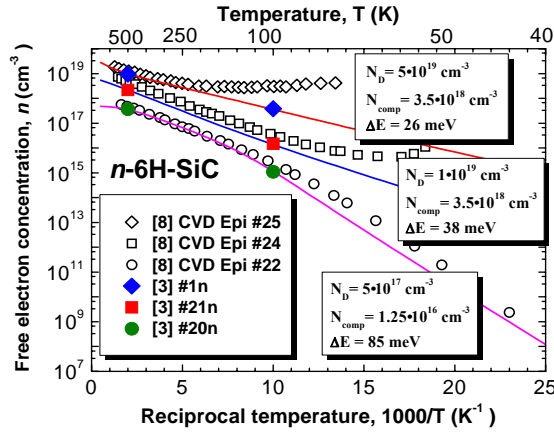


Fig. 6. Temperature dependence of the free electron concentration in *n*-6H-SiC. The line indicates the neutrality equation with presented parameters

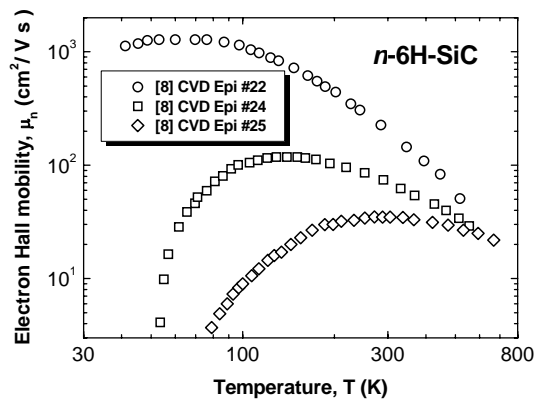


Fig. 7. Temperature dependence of the Hall mobility in *n*-6H-SiC

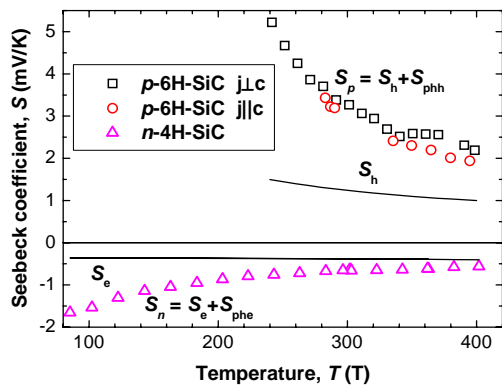


Fig. 8. Temperature dependence of the Seebeck coefficient in *p*-6H-SiC and *n*-4H-SiC

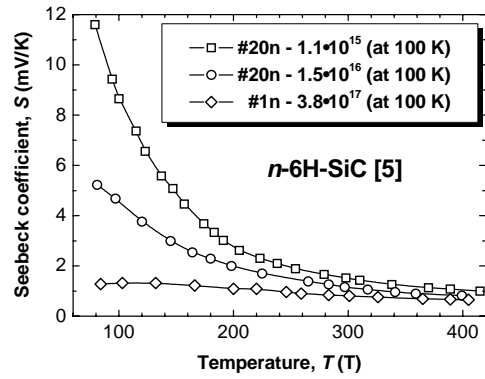


Fig. 9. Temperature dependence of the Seebeck coefficient in *n*-6H-SiC [5]

$$S_{e[h]} = \mp \frac{k_B}{|e|} \left( \frac{5}{2} + s + \ln \frac{N_{c[v]}}{n[p]} \right), \quad (1)$$

where  $k_B$  is the Boltzmann constant,  $s$  is the exponent in the relation between free carrier relaxation time and its energy

( $\tau \propto \varepsilon^s$ ) which depends on the scattering mechanism,  $N_{c[v]}$  is the effective density of states in the conduction [valence] band and  $n[p]$  is the concentration of free electrons [holes]. As it is mentioned above we reasoned that the main free carrier scattering mechanism in our *n*-4H-SiC and *p*-6H-SiC is ionized impurity and acoustic phonon scattering, respectively. Therefore, parameters in Eq. (1) has been adopted as 3/2 and -1/2 for *n*-4H-SiC and *p*-6H-SiC, respectively. The electronic part of the Seebeck coefficient is shown in Fig. 8 by lines. One can see that  $S_{e[h]}$  makes up only a small part of the whole Seebeck coefficient especially at low temperature.

### Phonon drag effect

The temperature  $S_{ph}$  dependencies obtained as a difference of  $S$  and  $S_{e[h]}$ . Phonon part of the Seebeck coefficient can be expressed as [3, 17]:

$$S_{ph} = K \frac{\bar{s}_l l_{ph}}{T \mu_{ac}}, \quad (2)$$

where  $\bar{s}_l$  is the average longitudinal sound velocity,  $l_{ph}$  is the mean free path of the long-wavelength phonons,  $\mu_{ac}$  is the free carrier mobility controlled by acoustic phonons scattering and  $K$  is the correction factor which depends on the free carries and phonon energy relaxation times. Sound velocity and temperature are two well-defined parameters. Since not only acoustic phonon but also other scattering mechanisms control the mobility [11], only the lower limit of the  $\mu_{ac}$  can be evaluated from the experimental results. It should be note than exclusively long-wavelength phonons (also called nonperipheral [18]) are able to interact with electrons. Their wave vector  $q_{ph} \leq 2q_{e[h]}$  where  $q_{e[h]}$  is the electron [hole] wave vector. Only these long-wavelength phonons must be taken into consideration during thermopower simulation.

It is assumed that different relaxation processes make a separate and independent contribution to the overall mean

free phonon path, i.e.,  $l_{ph}^{-1} = \sum_i l_{ph_i}^{-1}$ . The main phonon relaxation processes are as follow: (1) normal three-phonon, (2) Umklapp process, (3) boundary scattering, (4) impurity (including isotope) scattering, (5) charge carrier scattering and (6) four-phonon process. Herring in his seminal papers [1, 19] proposed two relaxation mechanism for long-wavelength phonons, namely, normal three-phonon process and boundary scattering. The boundary scattering is dependent on the sample dimensions and play significant role only at very low temperature [20, 21]. Thus this mechanism of relaxation is omitted from our calculation. As one can see in Fig. 9 the strength of phonon drag effect strongly depends on free carrier concentration. The larger  $n$  the smaller  $S_{ph}$ . Therefore, for the first step in the simulation of the process relatively low-doped samples ( $p$ -6H-SiC and  $n$ -6H-SiC # 20n) have been chosen.

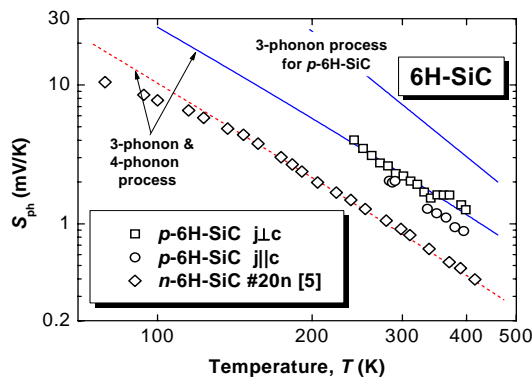


**Fig. 10.** Phonon Seebeck coefficient part vs. temperature. Points are experimental values. Curves represent theoretical calculation

As one can see in Fig. 10 simulation of the Seebeck coefficient phonon part using normal three-phonon process cannot described the experimental results of  $p$ -6H-SiC. It may be assumed that too high theoretical values of  $S_{ph}$  indicates that some additional phonon scattering mechanism is not taken into consideration. The doping of the samples shown in Fig. 10 is quite low so it is difficult to suggest that phonon drag effect is restricted by impurity or free carrier scattering. One of the possible phonon relaxation mechanism can be the four-phonon process proposed by Pomeranchuk [22] especially since it was shown that the inclusion of this process is necessary for stimulation of thermal conductivity in SiC [23]. The coefficient  $a_{4ph}$  for mean free phonon path associated with four-phonon process has been taken from the best fitting of temperature lattice heat conductivity dependence for low doped SiC [17] and is equal to  $1.5 \times 10^{-22}$  s/K. The inspection of Fig. 10 shows that theoretical curves obtained using normal three-phonon and four-phonon process for phonon relaxation is in a good agreement with experimental points. The distinction between calculated curve and measured points for  $n$ -6H-SiC increases with decreasing temperature from 110 K. Such behavior can be attributed to the influence of the boundary scattering. It is necessary to include phonon relaxation processes

associated with impurity and free carrier scattering into theoretical model describing Seebeck coefficient for higher doped SiC sample.

## CONCLUSIONS

The Seebeck coefficient temperature dependence of 4H- and 6H-SiC is presented. The main contribution to it for not too highly-doped sample gives part of  $S$  associated with phonon drag effect. Theoretical model including normal three-phonon and four-phonon processes into phonon relaxation makes possible correct simulation of the Seebeck coefficient temperature dependence for low-doped SiC. Any difference in the electrical characteristics of the  $p$ -6H-SiC samples parallel and perpendicular to  $\hat{c}$ -axis have not been perceived.

## Acknowledgments

The Swedish Royal Academy of Sciences and the Visby program are acknowledged for financial support.

## REFERENCES

1. **Herring, C.** The Role of Low-frequency Phonons in Thermoelectricity and Thermal Conduction. In: Halbleiter und Phosphore. Edited by M. Schön and H. Welker (Berlin), 1958: pp.184 – 235.
2. **Palmour, J. W., Singh, R., Glass, R. C., Kordina, O., Carter, Jr., C. H.** Silicon Carbide for Power Devices *IEEE Intern. Symp. Power Semic. Dev. & IC's ISPSD*, 1997: pp. 25 – 32.
3. **Grivickas, V., Stölzer, M., Velmre, E., Udal, A., Grivickas, P., Syväjärvi, M., Yakimova, R., Bikkajevras, V.** Thermopower Measurement in 4H-SiC and Theoretical Calculation Considering the Phonon Drag Effect *Mater. Sci. Forum.* 353 – 356 2001: pp. 491 – 494.
4. **Bikkajevras, V., Grivickas, V., Stölzer, M., Velmre, E., Udal, A., Grivickas, P., Syväjärvi, M., Yakimova, R.** Impact of Phonon Drag Effect on Seebeck Coefficient in  $p$ -6H-SiC: Experiment and Simulation *Mater. Sci. Forum.* 433 – 436 2003: pp. 407 – 410.
5. **Kirsons, J.** Thermoelectric Power and Transversal Nernst-Ettinghausen Effect in  $n$ -type Silicon Carbide *Izv. AN LatSSR. Ser. Fiz. Tech. Nauk* 3 1976: pp. 41 – 45 (in Russian).
6. **Syväjärvi, M., Yakimova, R., Tuominen, M., Kakanakova-Georgieva, A., MacMillan, M. F., Henry, A., Wahab, Q., Janzen, E.** Growth of 6H and 4H-SiC by sublimation epitaxy *J. Crystal Growth* 197 1999: pp. 155 – 161.
7. **Stölzer, M., Bechstein, V., Meusel, J.** Thermopower Measurement on Thin Films *Proc. 4<sup>th</sup> European Workshop on Thermoelectrics*, Spain, Madrid: Madrid University, 1998.
8. **Schöner, A., Karlsson, S., Schmitt, T., Nordell, N., Linnarsson, M., Rottner, K.** Hall Effect Investigation of 4H-SiC epitaxial layers Grown on Semi-insulating and Conducting Substrates *Mat. Sci. Eng. B* B61 – 62 1999: pp. 389 – 394.
9. **Choyke, W. J., Pensl, G.** Physical Properties of SiC *MRS Bulletin* March, 1997: pp. 25 – 29.

10. **Pensl, G., Choyke, W. J.** Electrical and Optical Characterization of SiC *Physica B* 185 1993: pp. 264 – 283.
11. **Iwata, H., Itoh, K. M., Pensl, G.** Theory of Anisotropy of the Hall Mobility in *n*-type 4H- and 6H-SiC *J. Appl. Phys.* 88 2000: pp.1956 – 1961.
12. **Sridhara, S. G., Clemen, L. L., Devaty, R. P., Choyke, W. J., Larkin, D. J., Kong, H. S., Troffer, T., Pensl, G.** Photoluminescence and Transport Studies of Boron in 4H SiC *J. Appl. Phys.* 83 1998: pp. 7909 – 7919.
13. **Addamiano, A., Potter, R. M., Ozarow, V.** *J. Electrochem. Soc.* 110 1963: p. 517.
14. **Schaffer, W. J., Negley, G. H., Irvine, K. G., Palmour, J. W.** Conductivity Anisotropy in Epitaxial 6H and 4H SiC *Mat. Res. Soc. Sym.* 339 1994: pp. 595 – 600.
15. **Itoh, A., Matsunami, H.** Single Crystal Growth of SiC and Electronic Devices *Critical Rev. Solid State & Mat. Sci.* 22 (2) 1997: pp. 111 – 197.
16. **Martinez, A., Lindefelt, U., Hjelm, M., Nilsson, H.-E.** Monte Carlo Study of Hole Mobility in Al-doped 4H-SiC *J. Appl. Phys.* 91 2002: pp. 1359 – 1364.
17. **Velmre, E., Udal, A.** Modeling of Lattice Heat Conductivity and Thermopower in SiC Considering the Four-Phonon Scattering Processes *Mater. Sci. Forum.* 433 – 436 2003: pp. 391 – 394.
18. **Blewer, R. S., Zebouni, N. H., Grenier, C. G.** Lattice Thermal Conductivity, Nernst-Ettinghausen Effect, and Specific Heat in Antimony at Low Temperature *Phys. Rev.* 174 1968: pp. 700 – 710.
19. **Herring, C.** Theory of Thermoelectric Power of Semiconductors *Phys. Rev.* 96 1954: pp. 1163 – 1187.
20. **Kaden, E., Günter, H.-L.** The Thermoelectric Power of *p*-Ge at Low Temperatures *Phys. Stat. Sol. (b)* 126 1984: pp. 733 – 740.
21. **Behnen, E.** Quantitative Examination of the Thermoelectric Power of *n*-type Si in the Phonon Drag Regime *J. Appl. Phys.* 67 1990: pp. 287 – 292.
22. **Pomeranchuk, I.** On the Thermal Conductivity of Dielectrics at the Temperatures Higher Than the Debye Temperature *J. Phys. (Moscow)* 4 1941: pp. 259 – 268.
23. **Joshi, R. P., Neudeck, P. G., Fazi, C.** Analysis of the Temperature Dependent Thermal Conductivity of Silicon Carbide for High Temperature Application *J. Appl. Phys.* 88 2000: pp. 265 – 269.